TEMPERATURE DEPENDENCE OF THE OPTICAL BAND GAP OF a-Si:H THIN FILMS

A THESIS SUBMITTED TO THE SCHOOL OF GRADUATE STUDIES
ADDIS ABABA UNIVERSITY

IN PARTIAL FULFILMENT OF THE REQUIREMENTS FOR THE DEGREE OF MASTER OF SCIENCE IN PHYSICS

BY
TESFAYE NEGASH

ADDIS ABABA
JUNE 1998

Acknowledgements

I am indebted to Dr. Ulrich Stutenbaeumer for his consistent advice, guidance and encouragement. Moreover I thank him for providing his own private materials for this work without reservation.

I would like to thank the physics department of the AAU for providing the necessary materials for this work. I wish to express my gratitude to Dr. Fesseha Kassahun for facilitating my work; Dr. Araya Asfaw for technical support and encouragement throughout my work and Ato Tadesse Tassew for technical support.

I extend my warmest gratitude to my friends Belayneh Mesfin and Tsegaye Abayneh for their encouragement and material support and to all my friends who encouraged and supported me in this work.

Finally I wish to thank the Southern Nations Nationalities People (SNNP) Educational Bureau for granting me the sponsorship to join the school of graduate studies in AAU.

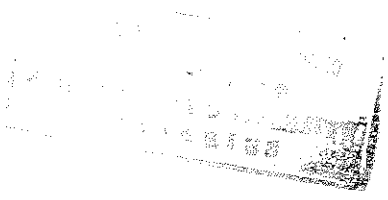

Contents

List of Tables

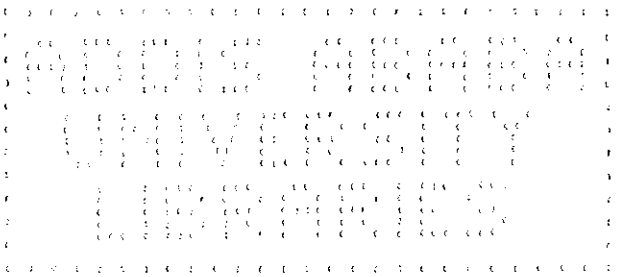

List of Figures

Abstract

The near normal incidence transmittance spectra of p-, i- and n-layer a-Si:H thin film samples, prepared by glow discharge decomposition of silane (SiH_4), were measured at two different temperatures (77 K and 300 K), for the first time at the Addis Ababa University. From the measured transmittance spectra the optical band gap of each a-Si:H thin film layer was calculated by computer simulation using the Forouhi and Bloomer dielectric function model which was derived for the interband transition of electrons. The effect of temperature on the optical band gap of a-Si:H thin films and hence on the solar cell application is discussed.

1. Introduction

A number of electronic applications of amorphous materials, almost all of semiconductors, have been proposed or put in to practice, especially since the discovery by Spear and Le Comber (1976) that a-Si:H could be doped either n-type or p-type by incorporating PH_3 or B_2H_6 in the silane (SiH_4) gas flow of a glow- discharge decomposition reactor [1].

The most technologically developed, and potentially the most important, application of amorphous semiconductor a-Si:H is the direct conversion of sun light to electrical power. The AM1 spectrum peaks at a wave length of 0.5 μm; which matches the absorption edge of a-Si:H better than that of crystalline Si. Since the band edge of a-Si:H is due to a direct optical transition, a film of a-Si:H only a few micrometers thick will absorb most of the useful sun light [1, 5].

The maximum energy conversion efficiency of a solar cell is fundamentally limited by the spectral width of the solar spectrum and by the optical absorption characteristics of the semiconductor material. In a wide band gap semiconductor there is little absorption, which results in a low efficiency. On the other hand, in narrow band gap semiconductors, most of the absorbed solar energy produces heat, which also results in low efficiency [2]. One of the requirements for optimum use of photovoltaic semiconductor devices is then, that the absorption should match the solar spectrum. Then the knowledge of the optical band gap is an essential prerequisite for the detailed understanding of the optical and electrical properties of a-Si:H thin films.

The region of greatest interest in semiconductor physics is the top of the valence band and the bottom of the conduction band. The reason for this is, that thermal excitation and optical

excitation (infrared, visible, UV) can only lift electrons across the gap, which is about 1.7 eV wide in amorphous silicon [3].

To see the effect of temperature on the optical band gap of a-Si:H films the transmittance of the samples were measured at two different temperatures (77 K and 300 K) for p-, i- and n-layer a-Si:H thin films. The p-, i- and n-layers are the main components of a p-i-n solar cell. The optical and electrical properties of semiconductors depend on temperature. The knowledge of the dependence on temperature of the optical band gap and other optical and electrical properties of a-Si:H thin films is important for the optimisation of solar cells. As the temperature of a solar cell increases the short circuit current J_{sc} increase and the open circuit voltage V_{oc} decrease due to the temperature shift of the optical band gap [4, 20].

The calculation of the optical band gap from the measured transmittance spectra is done by computer simulation using the SCOUTFIT program which applies the Forouhi and Bloomer dielectric function model. Forouhi and Bloomer derived an expression for the extinction coefficient k and refractive index n, for amorphous semiconductors, as a function of energy based on the quantum mechanical theory of absorption for interband transition. Using the SCOUTFIT program with the Forouhi and Bloomer dielectric function model is then an effective and efficient way of determining the optical band gap of a-Si:H thin films from the experimentally determined transmittance spectra.

2. Density of States in Amorphous Silicon

If a solid is formed by slowly decreasing the inter atomic distance, a, of a large number, N, of atoms, the N individual and discrete atomic energy states will interact and broaden into bands [3]. If we consider the case of a tetrahedral semiconductor (a-Si) having an atomic configuration s^2p^2, the atomic levels hybridize to form four sp^3 molecular hybrids each of which may admit a bonding or antibonding orbital; solid state interactions, then broaden the molecular levels into bands separated by a band gap (Fig. 2.1) [1].

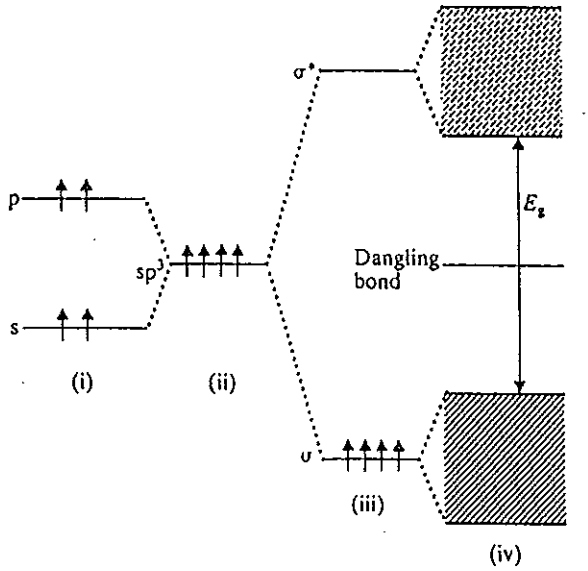

Fig. 2.1 Schematic representation of the origin of valence and conduction band states for a tetrahedrally bonded semiconductor (i) atomic s- and p-states; (ii) sp^3-hybrid states; (iii) bonding (σ) and antibonding (σ^*) states; (iv) broadening of σ - and σ^*-states into valence band (VB) and conduction band (CB) [1].

All important properties of semiconductors are governed by the electron states near the top of the upper most filled band (the valence band) and near the bottom of the first empty band (the conduction band). The region of greatest interest in semiconductor physics is then the top of the valence band and the bottom of the conduction band. The reason for this is that thermal

excitation or optical excitation can only lift electrons across the energy gap which is 1.7 eV wide in amorphous Si [3].

In amorphous semiconductors there are localized tail states, which are the results of lack of long range ordering, extending from the top of the valence band and from the bottom of the conduction band into the gap (see Fig. 2.3). These localized tail states are weakened or modified band states. They do not conduct, a charge carrier trapped in such state has zero mobility.

As in crystalline silicon the nearest neighbors of amorphous silicon atoms will still be at the vertices of a tetrahedron, but there will be distortions of the bond angels at the second, third neighbors and so on. One will arrive at a distribution of the atoms where some of the chemical bonds can not be established for geometrical reasons. These are called 'dangling bonds' (see Fig. 2.2). The energy levels corresponding to the dangling bonds are near the energy gap center. Having one electron only, it is detectable by electron spin resonance measurement (ESR) [6].

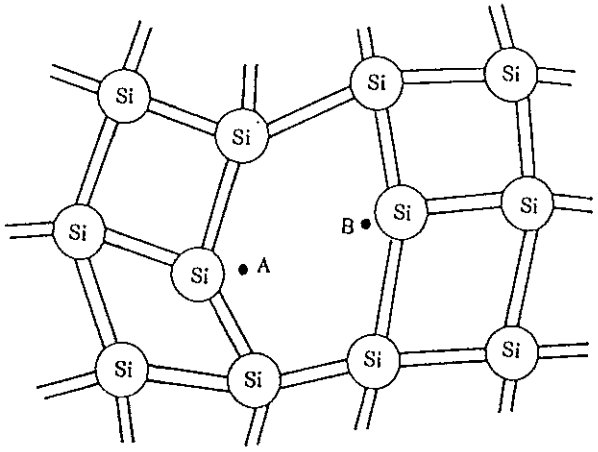

Fig. 2.2 Schematic representation of a disordered lattice of amorphous silicon. Most of the atoms establish four bonds, but because of the deformations, situations exist in which atoms A and B are too far apart to establish a bond [6].

It is believed that in amorphous silicon two bands of states in the energy gap are created by dangling bonds. One corresponding to single occupancy and the other corresponding to double occupancy. The second has an energy a few tenths of an eV higher than the other because of Coulomb repulsion between the two electrons. This energy difference is the so called electron correlation energy and it is positive in amorphous silicon [5].

An amorphous semiconductor, even though chemically pure, is thus "electronically" impure, since it has many states in the band gap as shown in Fig. 2.3. However, if we can replace the broken bonds with a strong chemical bond, each dangling bond we suppress will remove a state from inside the gap, the corresponding energy state now lying in the valance band [6]. When amorphous silicon is exposed to hydrogen at high temperatures, the hydrogen reacts and gives Si-H bonds, the corresponding states disappearing from within the band gap.

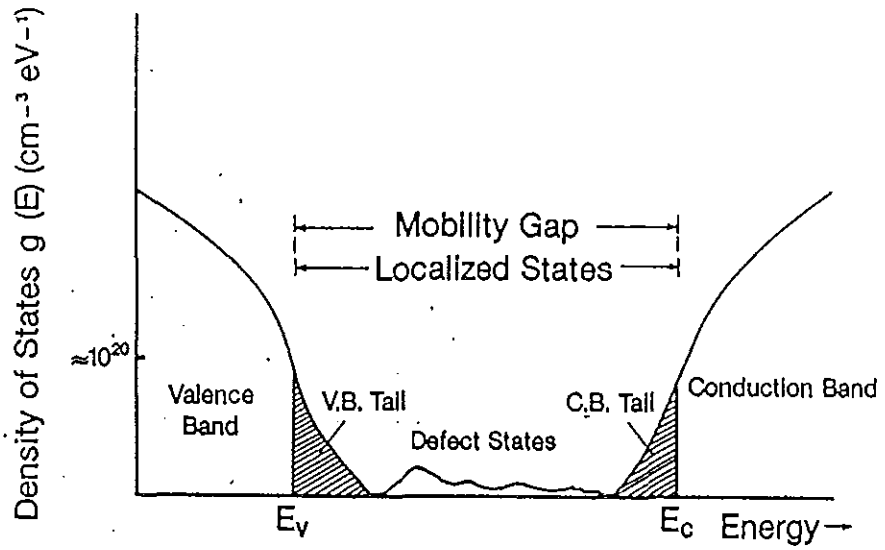

Fig. 2.3 Energy band model of a non crystalline semiconductor. E_v and E_c are the mobility edges of the valence band and of the conduction band, respectively [3].

3. Optical Properties of a-Si:H Solar Cells

3.1 Dielectric Function

The polarization $\vec{P}$ due to an electric field $\vec{E}$ in an isotropic linear medium is given by [7]

$$\vec{P} = \varepsilon_o \chi \vec{E} \qquad 3.1.1$$

where χ is the electric susceptibility and ε_0 is permitivity of free space, and the electric displacement is defined as

$$\vec{D} = \varepsilon_o \vec{E} + \vec{P} = \varepsilon_o (1 + \chi) \vec{E} = \varepsilon_m \vec{E} \qquad 3.1.2$$

where $\varepsilon_m = \varepsilon_o(1+\chi)$ is the permitivity of the medium. The relative permitivity or dielectric function is defined as

$$\varepsilon = \frac{\varepsilon_m}{\varepsilon_o} = (1 + \chi) \qquad 3.1.3$$

The relation ship between the electric displacement and the total electric field becomes

$$\vec{D} = \varepsilon_o \varepsilon \vec{E} \qquad 3.1.4$$

For a nonmagnetic medium the characteristics of the medium are contained in the parameters χ (or ε), which are functions of the optical frequency. They include the information necessary to describe dispersion and absorption.

3.2 Reflection and Transmission of Light at an Interface

The index of refraction, as well as the extinction and absorption coefficient can be related to the amplitude and polarisation of reflected and transmitted optical waves which can be measured directly. The relationship between these waves can be obtained from the boundary conditions at the interface between two media.

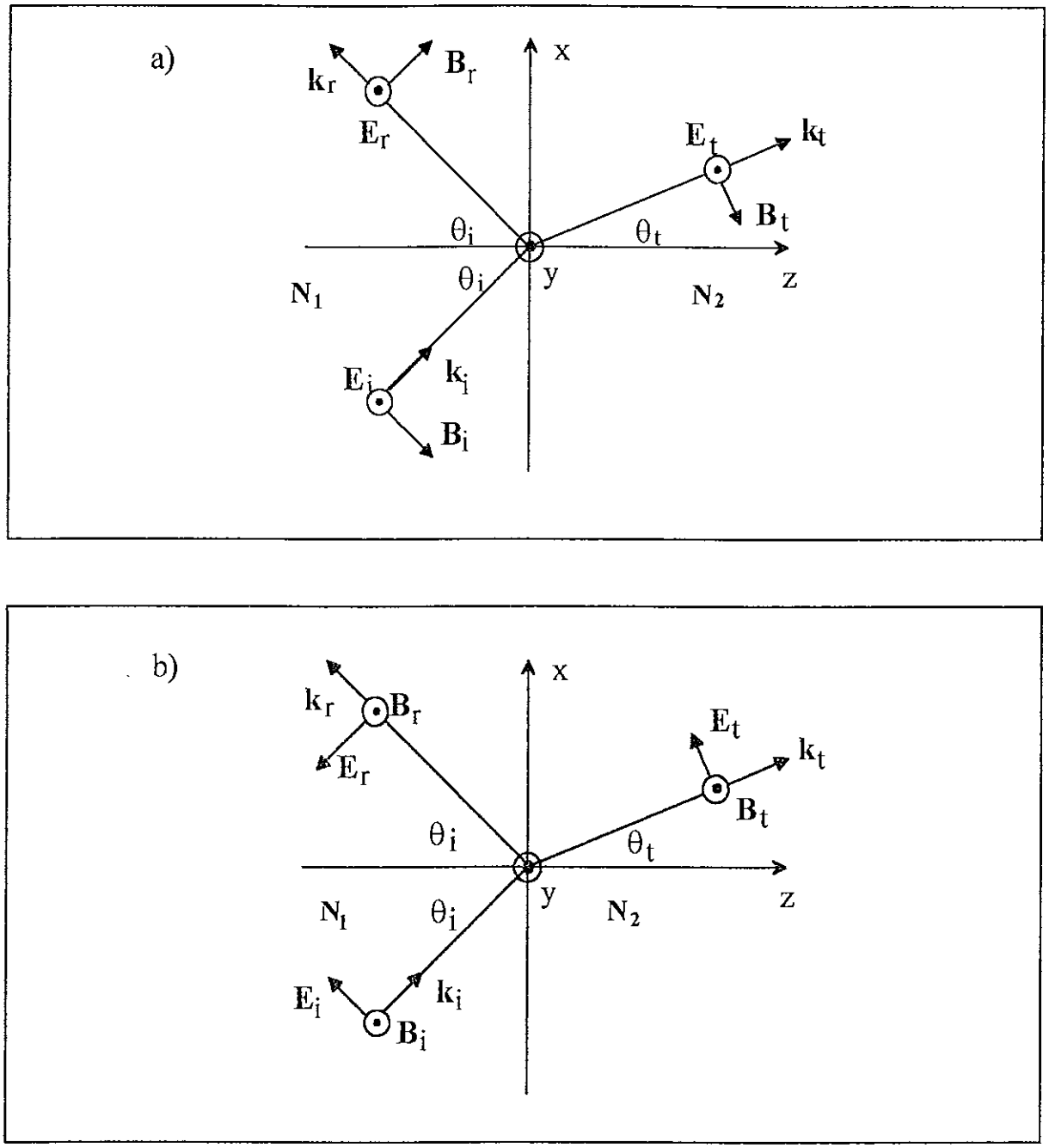

*Fig. 3.1 Light waves at an interface between two media with different refractive indices (a) **E** perpendicular to the plane of incidence (b) **E** parallel to the plane of incidence.*

Let the interface between two media having different optical properties lie in the XY plane shown in Fig. 3.1. The fields **E** and **B** may be resolved into their components in the plane of incidence and normal to the plane of incidence. Two independent cases then arise: the case **E** is perpendicular to the plane of incidence with **B** in the plane of incidence (s-polarization), and the case where **E** is in the plane of incidence with **B** perpendicular to it (p-polarization).

Reflection coefficient ρ and transmission coefficient τ are defined as [7]

$$\rho = \left|\frac{E_{or}}{E_{oi}}\right| \quad \text{and} \quad \tau = \left|\frac{E_{ot}}{E_{oi}}\right| \qquad 3.2.1$$

where E_{oi}, E_{or} and E_{ot} are the amplitudes of the incident, reflected and transmitted electric fields respectively.

In case of s-polarization the reflection and transmission coefficients are given by

$$\rho_s = \frac{N_1\cos\theta_i - N_2\cos\theta_t}{N_1\cos\theta_i + N_2\cos\theta_t} \qquad \tau_s = \frac{2N_1\cos\theta_i}{N_1\cos\theta_i + N_2\cos\theta_t} \qquad 3.2.2$$

where N_i is the complex refractive index of medium i and given by $N_i = n_i - ik_i$, here n_i is the real part of the refractive index and k_i is the extinction coefficient.

For normal incidence the s-polarization reflection and transmission coefficients become

$$\rho_s = \frac{N_1 - N_2}{N_1 + N_2} \quad \text{and} \quad \tau_s = \frac{2N_1}{N_1 + N_2} \qquad 3.2.3$$

In case of p-polarization the coefficients of reflection and transmission are

$$\rho_p = \frac{N_2\cos\theta_i - N_1\cos\theta_t}{N_2\cos\theta_i + N_1\cos\theta_t} \quad \text{and} \quad \tau_p = \frac{2N_1\cos\theta_i}{N_2\cos\theta_i + N_1\cos\theta_t} \qquad 3.2.4$$

For normal incidence this becomes

$$\rho_p = \frac{N_2 - N_1}{N_2 + N_1} \qquad \text{and} \qquad \tau_p = \frac{2N_1}{N_2 + N_1} \qquad 3.2.5$$

3.3 Energy Reflection and Transmission

The average pointing vector $\langle\vec{S}\rangle$ gives the time averaged power per unit area, and at the interface of nonmagnetic media it is given that [7]

$$\langle\vec{S}\rangle = n\frac{\varepsilon_o c}{2}\left|\vec{E}_o\right|^2\hat{s} \qquad 3.3.1$$

where n is the real part of N and $\hat{s}$ is a unit vector in the direction of propagation. The average power crossing a unit area of a plane surface parallel to the interface is given by the magnitude of the Z component of $\langle\vec{S}\rangle$, which is $\langle\vec{S}\rangle_Z = \langle\vec{S}\rangle\cos\theta$, thus we have for the three waves shown in Fig. 3 .1.

$$\text{Incident} \quad \langle \vec{S} \rangle_Z^i = \frac{\varepsilon_o c}{2} n_1 |E_i|^2 \cos\theta_i$$

$$\text{Reflected} \quad \langle \vec{S} \rangle_Z^r = \frac{\varepsilon_o c}{2} n_1 |E_r|^2 \cos\theta_i \qquad 3.3.2$$

$$\text{Transmitted} \quad \langle \vec{S} \rangle_Z^t = \frac{\varepsilon_o c}{2} n_2 |E_t|^2 \cos\theta_t$$

The reflectance R is defined by the ratio

$$R = \frac{\langle \vec{S} \rangle_Z^r}{\langle \vec{S} \rangle_Z^i} = \left| \frac{E_r}{E_i} \right|^2 = |\rho|^2 \qquad 3.3.3$$

and the transmittance T is defined by the ratio

$$T = \frac{\langle \vec{S} \rangle_Z^t}{\langle \vec{S} \rangle_Z^i} = \left| \frac{E_t}{E_i} \right|^2 \frac{n_2 \cos\theta_t}{n_1 \cos\theta_i} = |\tau|^2 \frac{n_2 \cos\theta_t}{n_1 \cos\theta_i} \qquad 3.3.4$$

For normal incidence

$$T = \frac{n_2}{n_1} |\tau|^2 \qquad 3.3.5$$

It can be shown that for both s- and p- polarizations T + R = 1 (if there is no absorption in the medium), which must follow from the conservation of energy.

For a semiconductor plate with two planar surfaces separated by a distance d, one must consider reflection from both surfaces as shown in Fig. 3.2.

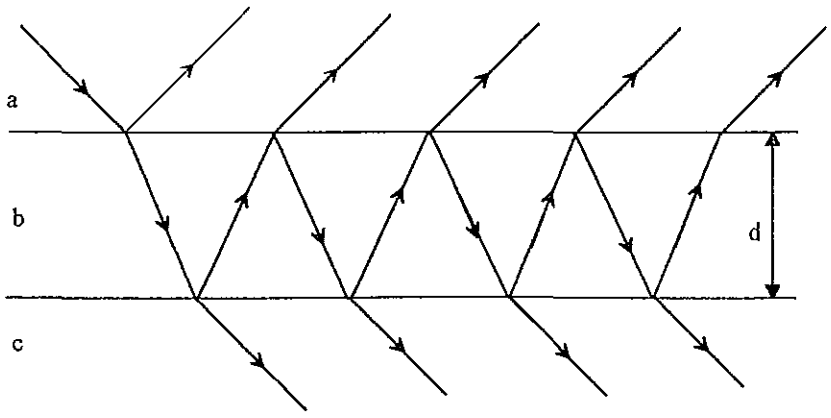

Fig. 3.2 Multiple reflection in a semitransparent slab.

Considering multiple reflections the amplitude reflection and transmission coefficients are obtained to be [8]

$$r_{a,b} = \rho_{a,b} + \frac{\tau_{a,b}\phi\rho_{b,c}\phi\tau_{b,a}}{1-\rho_{b,c}\phi\rho_{b,a}\phi} \quad , \quad t_{a,b} = \frac{\tau_{a,b}\phi\tau_{b,c}}{1-\rho_{b,c}\phi\rho_{b,a}\phi} \qquad 3.3.6$$

where $\phi = \exp(i\frac{\omega}{c_o}Nd)$, c_o is the speed of light in vacuum, ω is the angular frequency of light and N the complex refractive index of the slab.

The reflectance R and transmittance T are then given by

$$R = |\rho_{a,b}|^2 + \frac{|\tau_{a,b}|^2|\phi|^2|\rho_{b,c}|^2|\phi|^2|\tau_{b,a}|^2}{1-|\rho_{b,c}|^2|\phi|^2|\rho_{b,a}|^2|\phi|^2} \qquad 3.3.7$$

$$T = \frac{|\tau_{a,b}|^2|\phi|^2|\tau_{b,c}|^2}{1-|\rho_{b,c}|^2|\phi|^2|\rho_{b,a}|^2|\phi|^2}$$

3.4 Light Absorption in Amorphous Semiconductors

The optical absorption of a material is defined by the spectral dependence of its complex index of refraction, $\mathbf{N}(E) = n(E) - \mathbf{i}k(E)$ or the complex dielectric function $\varepsilon(E) = \varepsilon_1(E) - \mathbf{i}\varepsilon_2(E)$, where n is the refractive index and k is the extinction coefficient. ε is related to N by $\varepsilon = \mathbf{N}^2$, so that ε_1 and ε_2 can be determined from the knowledge of n and k. $\varepsilon_1 = \mathbf{n}^2 - \mathbf{k}^2$ and $\varepsilon_2 = \mathbf{2nk}$. In addition to k and ε_2, which relate to absorption of light, the absorption coefficient α is also used to describe absorption. The optical absorption coefficient α is related to k and ε_2 by the following relations, $\alpha = \mathbf{2}\omega\mathbf{k}/\mathbf{c}$ and $\varepsilon_2 = \mathbf{nc}\alpha/\omega$, where ω represent the photon frequency and c the speed of light [9, 10].

The spectral region of major interest for a semiconductor is in the vicinity of the absorption edge, since it provides information on the optical band gap as well as the density of states

within the energy band gap. For semiconductors, n and k are usually obtained from transmission and reflection measurements.

Quantum statistics applies equally to electrons in crystalline and noncrystalline materials. Therefore, there is a Fermi energy E_F below which the energy states are occupied by electrons in equilibrium. Essentially no electronic optical excitation can occur unless the photon energy hv exceeds a threshold energy that is large enough to lift an electron from the valence band (E_V) to an empty state above E_F or from an occupied state below E_F to the conduction band (E_C). These gap state to band state (G - B) transition starts at the threshold energy for photoconductivity. At higher photon energies hv, transitions between tail states and band states (T - B) occur, and at even higher photon energies band to band (B - B) transitions take place (Fig. 3.3) [3].

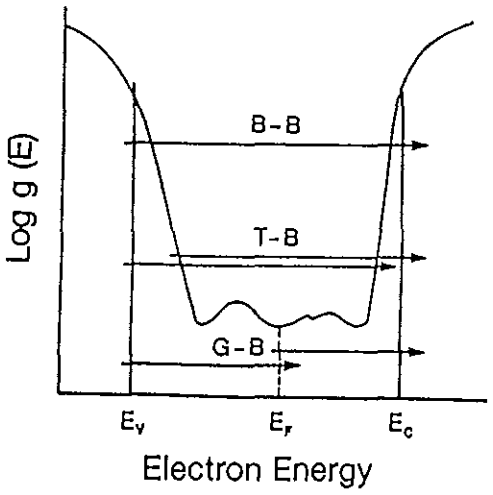

Fig. 3.3 Optical absorption processes: B - B between extended band states; T - B between tail states and band states; and G - B between gap states and band states [3].

For tetrahedrally-bonded amorphous semiconductors the optical absorption spectrum can be divided in to three regions; the high absorption region in the range of $10^3 < \alpha < 10^5$ cm^{-1},

where the optical band gap E_g is determined from the Tauc plot, the exponential part for which $10^0 < \alpha < 10^3$ cm^{-1} and the weak absorption tail where $\alpha < 10^0 \sim 10^1$ cm^{-1} (see Fig. 3.4) [11].

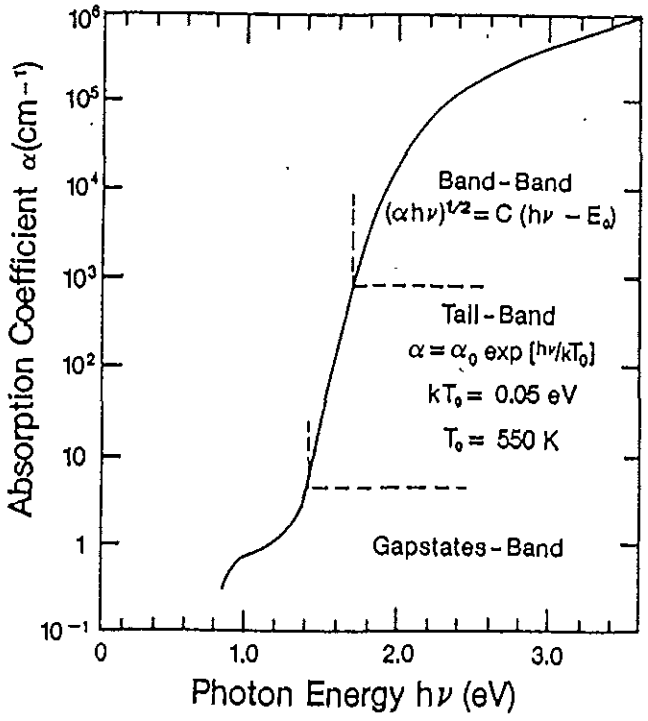

Fig. 3.4 Absorption spectrum of hydrogenated amorphous silicon (a-Si:H) [3].

Considering that portion of absorption occurring at photon energies corresponding to the band gap energy for amorphous semiconductors, it is assumed that the densities of states just beyond the mobility edges can be expressed in power law form as [1, 4]

$$g_v(-E) \sim E^p \qquad 3.4.1$$

$$g_c(E) \sim (E - E_o)^q \qquad 3.4.2$$

where energies are measured from the valance band mobility edge and E_o marks the mobility edge in the conduction band (i.e. it is the magnitude of the mobility gap).

For amorphous semiconductors the imaginary part of the dielectric constant ε_2 in a one electron expression is given by [1]

$$\varepsilon_2(\omega) = 2\left(\frac{2\pi e}{m\omega}\right)^2 a^3 P_{cv}^2 \int_0^{h\omega} dE g_v(-E) g_c(\hbar\omega - E) \qquad 3.4.3$$

where a is interatomic spacing and e, m and P_{cv} are the electron charge, mass and momentum respectively.

We see from 3.4.3 that $\varepsilon_2(\omega)$ is a function of a joint density of valence and conduction band states. Inserting 3.4.1 and 3.4.2 in 3.4.3 gives [1, 4]

$$\omega^2 \varepsilon_2(\omega) \propto (\hbar\omega - E_o)^{p+q+\frac{1}{2}} \qquad 3.4.4$$

If the form of the densities of states at both band edges is parabolic i.e. p = q = 1/2, the photon energy dependence of the absorption becomes

$$\omega\alpha(\omega) \propto \omega^2 \varepsilon_2(\omega) \propto (\hbar\omega - E_o)^2 \qquad 3.4.5$$

For photon energies comparable to the energy gap E_g, the above results show that interband transition give rise to a power law behaviours of the optical absorption coefficient $\alpha(\omega)$.

If the interband absorption mechanisms were the only ones operating, we would expect a rather sharp 'absorption edge' marking the onset of optical transitions (at energy corresponding, say, to $\alpha(\omega) \cong 10^4$ cm^{-1}), much as is observed in crystalline semiconductors. Instead, amorphous semiconductors almost always exhibit an absorption edge which is considerably less sharp and which consequently tails well into the energy gap as shown in Fig. 3.5, and which invariably obeys an exponential dependence on photon energy [12].

$$\alpha(\omega) = \alpha_o \exp\left[\frac{\hbar\omega - E_1}{E_e}\right] \qquad 3.4.6$$

where E_1 is an energy comparable to the threshold energy E_g involved in interband transition and E_e is a temperature-dependent constant.

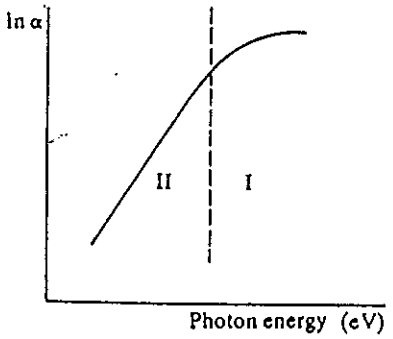

Fig. 3.5 Schematic illustration of optical absorption in amorphous semiconductors showing the interband region (I) and the Urbach edge region (II) [1].

3.5 Forouhi and Bloomer Dielectric Function Model

Based on quantum-mechanical theory of absorption Forouhi and Bloomer deduced a general expression for the extinction coefficient k for amorphous semiconductor. The optical energy gap, E_g, is identified to be that energy for which k(E) has its absolute minimum. From the deduced equation of k(E) then they derived an expression for the refractive index, n(E), via Kramers-Kronig dispersion relation.

For particular photon energies, peaks occur in the optical spectra. These peaks are attributed to transitions of electrons from one distinguishable state to another. These states are defined as either bonding, $|\sigma\rangle$, and antibonding, $|\sigma^*\rangle$, states in the valence and conduction bands of amorphous materials. In the simplest case of amorphous semiconductors and dielectrics a single peak is exhibited in the optical spectra, implying only one possible type of distinguishable transitions, from $|\sigma\rangle$ to $|\sigma^*\rangle$.

In the fundamental optical regime, interband transitions of bound electrons are mostly responsible for optical properties. Therefore, considering the relationship between photon absorption and electron transitions the extinction coefficient is obtained to be [13]

$$k(E) = \frac{A(E - E_g)^2}{E^2 - BE + C} \qquad 3.5.1$$

where: $A = const|\langle\sigma^*|\vec{X}|\sigma\rangle|^2 \times \gamma$,

$B = 2(E_{\sigma^*} - E_\sigma)$,

$C = (E_{\sigma^*} - E_\sigma)^2 + \frac{h^2\gamma^2}{8\pi}$.

$|\langle\sigma^*|\vec{X}|\sigma\rangle|^2$ represents the dipole matrix element squared between bonding, $|\sigma\rangle$, and antibonding, $|\sigma^*\rangle$, states and $\vec{X}$ is the electron position vector. $\gamma = 1/\tau$, where τ is the life time of the electron in the excited state.

Based on the relation of the refractive index, n(E), and the extinction coefficient, k(E), by the Kramers-Kronig relations they obtained an expression for the refractive index as:

$$n(E) = n(\infty) + \frac{B_\alpha E + C_\alpha}{E^2 - BE + C}, \qquad 3.5.2$$

where: $B_\alpha = \frac{A}{Q}\left(-\frac{B^2}{2} + E_g B - E_g^2 + C\right)$,

$C_\alpha = \frac{A}{Q}\left[\left(E_g^2 + C\right)\frac{B}{2} - 2E_g C\right]$.

$n(\infty) = \lim_{E\to\infty} n(E)$

and $Q = \frac{1}{2}(4C - B^2)^{\frac{1}{2}}$

The energy dependency of both k(E) and n(E), given by Equations 3.5.1 and 3.5.2, can be fully and simultaneously determined by five parameters, A, B, C, E_g and $n(\infty)$.

The value of B/2 is approximately equal to the energy at which k(E) is maximum. This is because k(E) is close to a maximum when $h\nu \cong E_{\sigma^*} - E_\sigma = B/2$. The parameter C depends on the energy difference between distinguishable states and on the life time of a distinguishable transition.

4. Optical Band Gap Dependence on Temperature

It is known that the band gap of semiconductors changes with temperature. The observed change in the band gap is due to the shift of the band edges, i.e. the shift of the conduction band E_c and the valence band E_v. This effect has two origins: The first is the thermal expansion of the structure, which produces a change in the one-electron potential; the other is electron-phonon coupling via Debye-Waller and self-energy correction. The band gap usually decreases with increasing temperature (see Fig. 4.1).

The temperature dependence of the energy gap over a large temperature range can be approximated by [14]:

$$E_g = E_{g0} - \frac{\alpha T^2}{\beta + T} \qquad 4.1$$

where E_{g0} is the band gap at T = 0 K and α and β are constants.

The temperature dependence of the optical band gap of hydrogenated amorphous silicon has the form [15]:

$$E_g = E_{g0} - \xi T \qquad 4.2$$

ξ is typically in the 10^{-4} eV/K range. For lower temperatures, however, ξ decreases and vanishes for T tending to zero according to the third law of thermodynamics.

For a-Si:H type alloys Cody et al. [16] have concluded that both the Urbach tail and the optical gap are controlled by the amount of structural and thermal disorder in the network. Further they concluded that hydrogen affects the band gap only indirectly.

The exponential dependence of the absorption coefficient $\alpha(E,T)$ can be expressed by the Urbach form as

$$\alpha(E, T) = \alpha_0 \exp[\frac{(E - E_1)}{E_e(T, X)}] \qquad 4.3$$

where $E_e(T,X)$ is the width of the exponential tail, X is a parameter that defines the structural disorder. α_0 and E_1 are experimentally determined parameters with values of 1.3 x 10^6 cm^{-1} and 2.2 eV, respectively. By fitting outside the exponential region ($\alpha > 10^4$ cm^{-1}) they obtained the temperature dependence of the optical energy gap given by:

$$[\alpha(E,T)E]^{\frac{1}{2}} = C[E - E_g(T)] \qquad 4.4$$

where C is a temperature independent constant equals 6.9 $(eV\mu m)^{-1/2}$

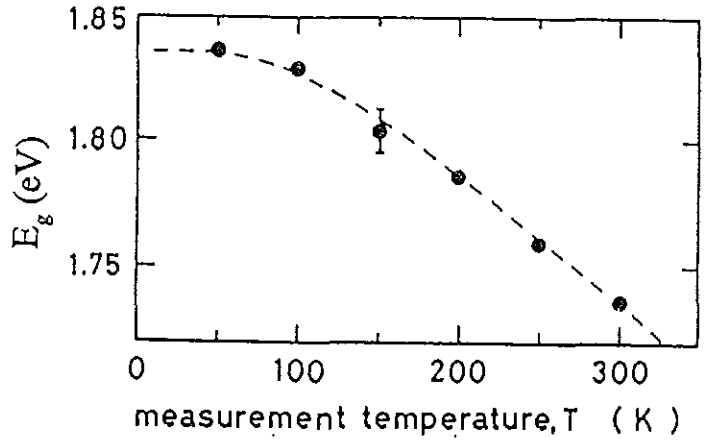

Fig. 4.1 Optical band gap as a function of temperature [11].

5. THIN Film a-Si:H Solar Cells

Photoelectronic devices such as solar cells, have been commercialised on the basis of the excellent photoconductivity of hydrogenated amorphous silicon (a-Si:H) prepared by the glow discharge plasma enhanced chemical vapour deposition (CVD) [17].

The most effective homojunction solar cells employing amorphous absorbers have been p-i-n amorphous silicon. In a p-i-n device construction a thin p^+ layer (10 nm - 30 nm) is first deposited on to a conducting substrate (ITO, SnO_2, etc.) followed by the deposition of an a-Si:H intrinsic layer (500 nm - 700 nm in thickness), and then by the deposition of a thin n^+-layer (<20 nm). The structure is completed with a metal reflector such as Ag or Al (see Fig. 5.1). In the p^+ layers which are generally fabricated from SiH_4 and B_2H_6 gas mixtures the band gap E_g is narrowed with the addition of B, and hence with increasing B doping the optical absorption of the p^+-layer increases. Hence, for cell configurations that utilise light entry through the p^+-type side, there is a loss of current in the device, especially at the blue end of the spectrum. To circumvent this a wide band gap amorphous material composed of Si:C:B:H has been developed using gas mixtures of SiH_4, CH_4, B_2H_6 and H_2. Materials with band gaps ranging in energy from 1.76 eV to 2.2 eV have been fabricated [12].

In a p-i-n type solar cell with light entering the p-side, optical enhancement or light trapping is achieved by scattering the incident light from the textured tin oxide and by reflecting light back into the cell from the rear contact. The tin oxide acts as a window to the incoming radiation and it serves as an ohmic contact to the p-layer. The rear metal contact makes an ohmic contact to the n-layer and it reflects the long wavelength light back to the cell [7].

The energy conversion efficiency, η, of a solar cell can be deduced from a knowledge of certain of its operating characteristics, and so is defined by the relation [1, 4, 12]

$$\eta = \frac{J_{sc} V_{oc} FF}{P_{in}} \qquad 5.1$$

where J_{sc} is the short circuit current density, V_{oc} is the open circuit voltage, P_{in} is the solar illumination intensity and FF is the 'fill factor' defined by the relation

$$FF = \frac{J_m V_m}{J_{sc} V_{oc}} \qquad 5.2$$

where J_m and V_m are the values of current density and voltage at the point of maximum power.

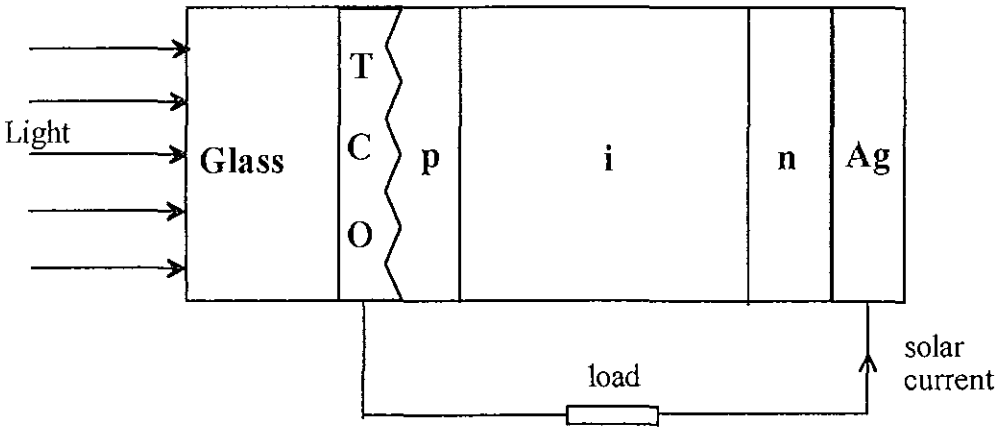

Fig. 5.1 Schematic structure of an a-Si:H p-i -n hetrojunction solar cell.

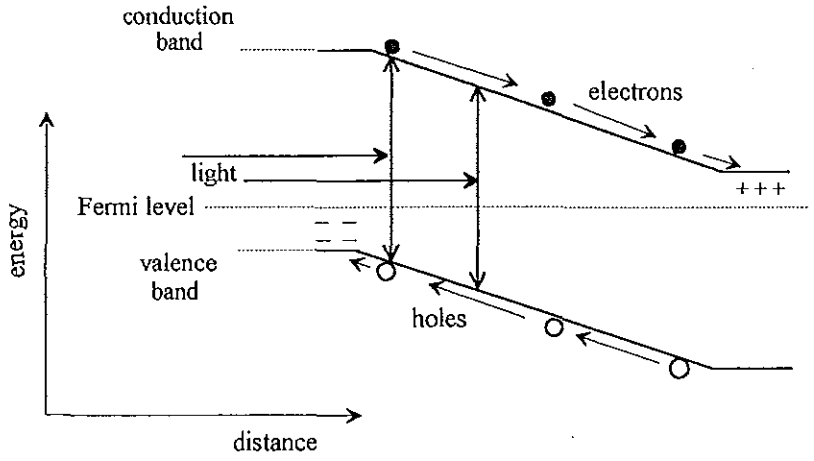

Fig. 5.2 Simplified band-diagram of a p-i-n solar cell.

6. Experimental Details

In this investigation the optical properties of different a-Si:H thin film layers are studied at two different temperatures, at room temperature (T = 300 K) and at the temperature of liquid nitrogen (T = 77 K). The transmittance of the samples were measured at the two temperatures at the near normal angle of incidence in the spectral range from 500 nm to 1050 nm. This is the spectral range which gives the most important information about the optical band gap of the investigated a-Si:H samples.

To measure the transmittance the sample was fixed in its holder in the cryostat (Fig. 6.2) and the film side is illuminated with light from an 80 W halogen lamp. The light from the lamp is focused by lenses onto the sample as shown in Fig. 6.1. The transmitted light is then detected by a Si p-i-n photodiode after passing through a grating monochromator with resolution of +/-0.0124 eV.

The transmitted light intensity is then measured as a function of wavelength with sample and without sample in the sample holder and the transmittance is calculated for each sample. From the measured transmittance spectra the optical constants are obtained by computer simulation with the SCOUTFIT program using the Forouhi and Bloomer dielectric function model.

6.1 Optical System

The optical system for the transmittance measurement at near normal angle of incidence is shown in Fig. 6.1. The light from an 80 W halogen lamp is focused by lenses L_1 and L_2 to the site of the sample in the cryostat. Lenses L_3 and L_4 are used to focus the transmitted light to the ORIEL Model 77250, 1/8 m monochromator, with an identical entrance and exit slits of width 760 μm. The resolution of the monochromator is then +/-0.0124 eV at 500 nm.

A Si p-i-n photodiode is mounted at the exit slit of the monochromator to detect the light through it. The detector has a sensitive area of 1 mm^2 and normalized detectivity of $D^* = 5x10^{12}\left[\frac{cm\sqrt{Hz}}{W}\right]$ and maximum sensitivity at 850 nm. The Si diode is electrically connected with an amplifier so that the signal current detected by the photodiode is amplified there and reading can be taken from a digital multimeter at the output of the amplifier.

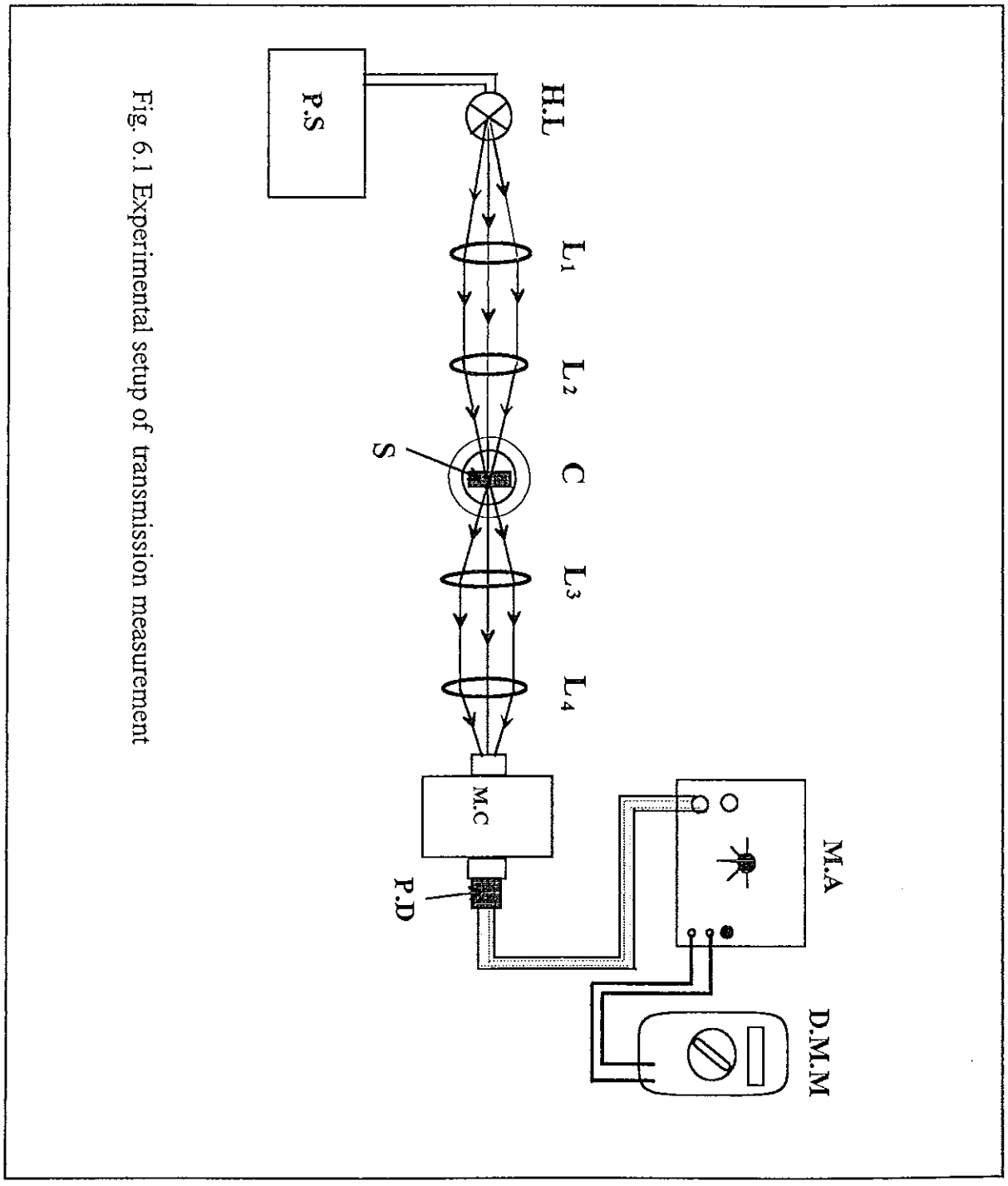

Fig. 6.1 Experimental setup of transmission measurement

Figure 6.1 shows the experimental set up for the transmittance measurement and the following notations are used. L_1, L_2, L_3 and L_4 represent lenses of focal length f_1 = 200 mm, f_2 = 100 mm, f_3 = 150 mm and f_4 = 50 mm, respectively. P.S: power supply; H.L: Halogen lamp; C: cryostat; S: sample; M.C: monochromator; M.A: measuring amplifier; P.D: photodiode; D.M.M: digital multimeter.

6.2 Samples

a-Si:H is most often produced by the glow discharge (GD) technique, this is important because of its device prospects in view of the fact that it can be readily doped. Silane (SiH_4) has long been the reactant gas used to produce a-Si:H with or without argon gas as diluent. This produces hydrogenated amorphous silicon (a-Si:H) films under optimum condition (with of the order of 5-10 at % H contained within the material). The a-Si:H materials doped either n-type or p-type by admitting phosphine (PH_3) or diborane (B_2H_6) respectively, into the silane gas stream; the dopant atoms are incorporated into the amorphous structure substitutionally, thereby liberating excess electrons (for phosphorus) or holes (for boron) [1].

The p-, i-, and n-layer thin film a-Si:H samples used in this investigation were prepared by a r.f glow-discharge (GD) decomposition of silane (SiH_4) in the Juelich research center (Germany). Each of this a-Si:H films were deposited on a glass substrate of thickness about 1.1 mm which was coated by a thin transparent conducting oxide (TCO) of thickness about 0.07 μm. The transmittance measurements were made for the samples listed in Table 6.1.

Table 6.1 List of the investigated a-Si:H thin film samples.

a-Si:H sample	thickness (nm)
i-layer	100
i-layer	1,000
p-layer	1,000
n-layer	1,000

6.3 The Liquid Nitrogen Bath Cryostat

In this investigation transmittance measurements at 77 K were performed using a glass tube cryostat shown in Fig. 6.2, which was constructed in the work shop of the Chemistry department (AAU). The cryostat was used to keep the nitrogen for a longer period of time in the liquid state while the transmittance measurements were taken. It was made up of a double walled glass tube of height about 40 cm. The region between the two walls of the tube is evacuated, this enables us to keep the liquid nitrogen longer in its liquid state with a temperature of T = 77 K in the cryostat by reducing the transfer of heat from the surrounding environment in to the liquid nitrogen. After pouring the liquid nitrogen into the cryostat it is sealed with a plastic fastener, which also host the sample holder and a small opening to let the evaporating nitrogen out of the cryostat as shown in Fig. 6.2.

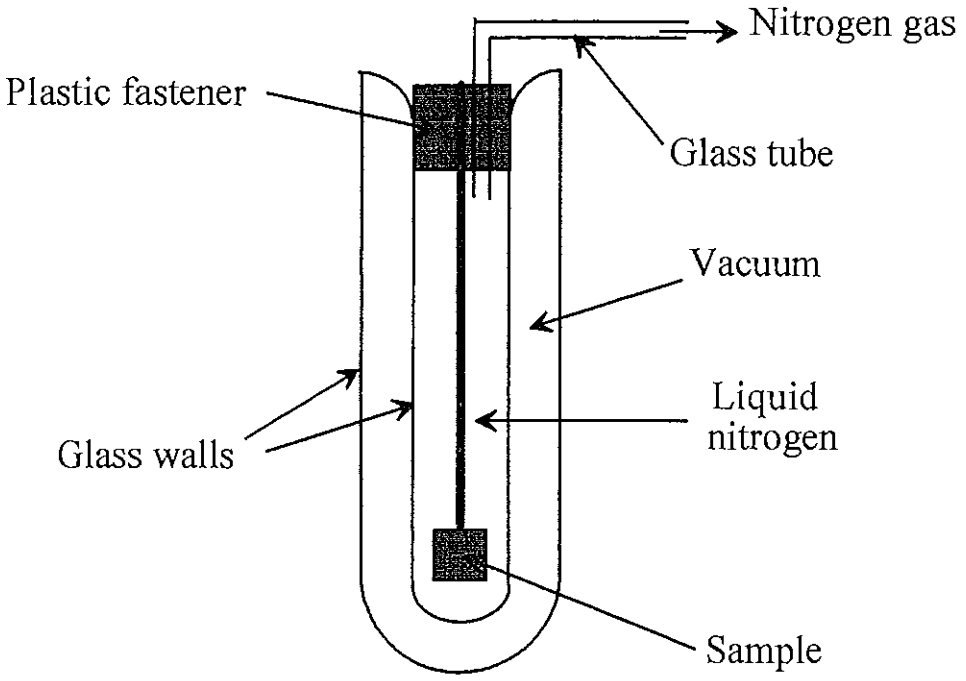

Fig. 6.2 Cross-sectional view of the cryostat.

6.4 Experimental Procedure

After arranging the optical system shown in Fig. 6.1 the out put signal was first optimised. This was achieved by looking for the maximum reading from the digital multimeter. Care has been taken to protect the saturation of the measuring amplifier.

To get the transmittance of the samples the spectrum of the halogen lamp was first measured without sample in the cryostat. This procedure is also repeated with liquid nitrogen in the cryostat. From this the intensity of the light, I_o, which illuminates the sample is obtained at room temperature when the cryostat is empty, and at 77 K when the cryostat is filed with liquid nitrogen. To measure the intensity of the light transmitted through the sample at 77 K the cryostat is first filled with liquid nitrogen and the sample is then put in the liquid nitrogen with its holder, such that the light from the lamp illuminates the film side of the sample perpendicularly. The intensity of the transmitted light, I_t, is then determined by the reading of

the multimeter as a function of wavelength. The wavelength of the monochromator can be changed by a hand wheel. From the measured values of I_o and I_t the transmittance T is calculated for each sample using $T = I_t / I_o$ [19].

7. Data Analysis

The transmittance data collected using the procedure discussed in Chapter 6 were analysed using a SCOUTFIT program. The SCOUTFIT program is a windows application for computer assisted optical spectroscopy (CAOS) which is an approach to the interpretation of optical spectra by computer simulation. CAOS is a method based on a rearrangement of the measured data to quantities that can easily be interpreted [8].

In many cases it is not possible to transform measured spectra directly into some quantities that carries quantitative information. However the simulation approach has turned out to be a reliable solution as long as reasonable models are used with an appropriate number of adjustable parameters. A direct simulation of optical spectra has to be based on the macroscopic response of matter to electric fields which is given by the dielectric function of a material.

The SCOUTFIT simulation with the Forouhi and Bloomer dielectric function model is an efficient and accurate method for the determination of optical band gaps of a-Si:H thin film samples. For the analysis of the transmittance data a model for interband transitions was used. Forouhi and Bloomer proposed a dielectric function model for interband transitions (Section 3.5). The parameters A, B, & C in the original expressions of the Forouhi and Bloomer model are not very useful for a fit to experiments. Therefore A, B, & C are replaced by three new parameters A, position and delta (δ). The parameter A is the same as in the original publication. The parameter position equals B/2 and is the wave number position where the imaginary part of the dielectric function shows a peak and delta equals $[C - (B/2)^2]^{1/2}$ [8].

To obtain the optical band gap of the p-, i- and n-layers of a-Si:H films from the measured transmittance using the SCOUTFIT program initial fit parameters were used (Fig. 7.1). With

the help of Fresnels equations the program calculates a simulated transmittance spectrum and compares it with the measured one. By changing the initial parameters the program again calculates for a better simulated transmittance spectrum. This iterative calculation continues by replacing the simulated spectrum with another of smaller deviation compared to the measured transmittance spectrum [20]. The parameters used in this iterative calculation for each layer of the samples are listed in Table 7.1.

Table 7.1 List of SCOUTFIT parameters defined for each layer of the samples.

layer	SCOUTFIT parameters
i-, p-, n-	A, delta (δ), position, n_{inf}, E_g, layer thickness (d)
TCO	Dielectric constant, layer thickness (d)
Glass	Dielectric constant, layer thickness (d)

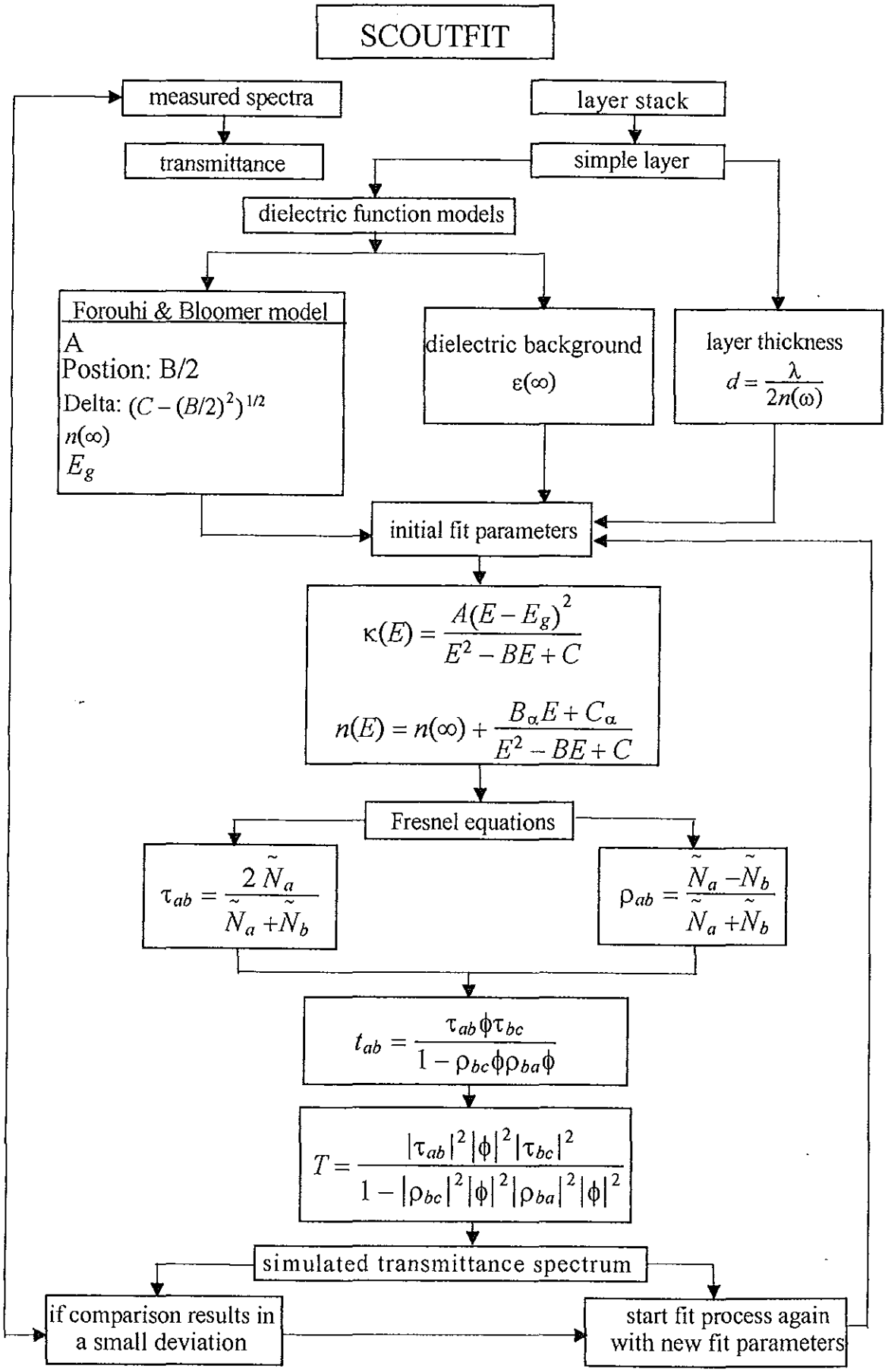

Fig. 7.1 The fitting process in the SCOUTFIT computer program.

8. Results and Discussion

The design of hydrogenated amorphous silicon (a-Si:H) p-i-n solar cells require the understanding of the optical properties of their individual layers. Additionally, the knowledge of the optical band gap of each layer is important for the further improvement of the efficiency of thin film solar cells.

For the GD a-Si:H samples of p-, i-, and n-layers transmittance was measured as discussed in Chapter 6 at two different temperatures, 77 K and 300 K. By simulation using the SCOUTFIT computer program with the Forouhi and Bloomer dielectric function model the optical band gaps E_g of the samples were determined from the measured transmittance spectra . Since the Forouhi and Bloomer model is derived for interband transition of electrons, the simulation was restricted near the expected optical band gaps of the sample layers.

The transmission spectra of the a-Si:H samples show complete absorption in the UV region due to the absorption by the glass substrate since it has a wide optical band gap. In the visible region, where the energy of light corresponds to the optical band gap energy of a-Si:H, strong absorption in the transmission spectra takes place. This strong absorption is caused by the band to band transition. For the infrared (IR) region the photon energy becomes less than the optical band gap E_g, as a result only weak absorption can be observed in this region, and the samples become almost transparent in the IR spectral region.

The transmittance spectra of a-Si:H films of thickness 1000 nm display a number of interference fringes in the region where there is weak absorption. But in the transmittance spectra of the thin i- layer sample of thickness 100 nm only one interference peak is seen in the given spectral region. This difference arises because of the dependence of the periodicity of the interference fringes on the thickness of the films. Generally, the periodicity of

interference fringes is inversely proportional to the thickness and refractive index of the film. Thicker samples will have more interference fringes in a given spectral range than the thinner ones.

8.1 The Effect of Temperature on the Transmittance Spectra

After illuminating the same sample spot at two different temperatures, 77 K and 300 K, the transmission spectra obtained are shown in Figs. 8.1 to 8.4 for i-, p-, and n-layers of a-Si:H thin films.

In Fig. 8.1 the transmittance spectra of a thin i-layer a-Si:H film of thickness 100 nm is shown for the two temperatures, 77 K and 300 K. The transmittance spectrum at 300 K is shifted towards lower energies compered to the spectrum for 77 K. This accounts for the shift of the optical absorption edge to lower energies with increasing temperature. The shift seen in the transmission spectrum for this sample is about 0.09 eV. The sharp drop in the transmission below 1.6 eV could be due to the interference effect and not to a real absorption process.

The transmittance spectra of the thick i-layer sample of thickness 1000 nm is shown in Fig. 8.2 at 77 K and 300 K. Since this film is thicker than the one depicted in Fig. 8.1, a number of interference peaks in the transmittance spectra at both temperatures can be seen. Additionally, the shift of the transmittance curve towards lower energies with increasing temperature can be observed. In the energy range from around 1.65 eV to 2.1 eV transmission is high at the lower temperature (77 K) compered to the higher temperature (300 K) spectrum due to the shift of the optical band edge towards higher energies with decreasing temperature. In the region of strong absorption the observed maximum temperature shift is about 0.08 eV.

Figure 8.3 shows the transmittance spectra of a p-layer a-Si:H film of thickness about 1000 nm at the two temperatures (77 K and 300 K). In the region of strong absorption the temperature shift of the transmittance spectra is about 0.05 eV. Also an increased

transmission with decreasing temperature in the region of energy corresponding to the optical band gap can be observed.

The transmittance spectra for the n-layer a-Si:H thin film shown in Fig. 8.4 also displays the shift of the transmission spectrum towards lower energies with increasing temperature. In this case the temperature shift in energy of the transmission spectrum is about 0.051 eV in the energy range corresponding to the optical band gap of the film.

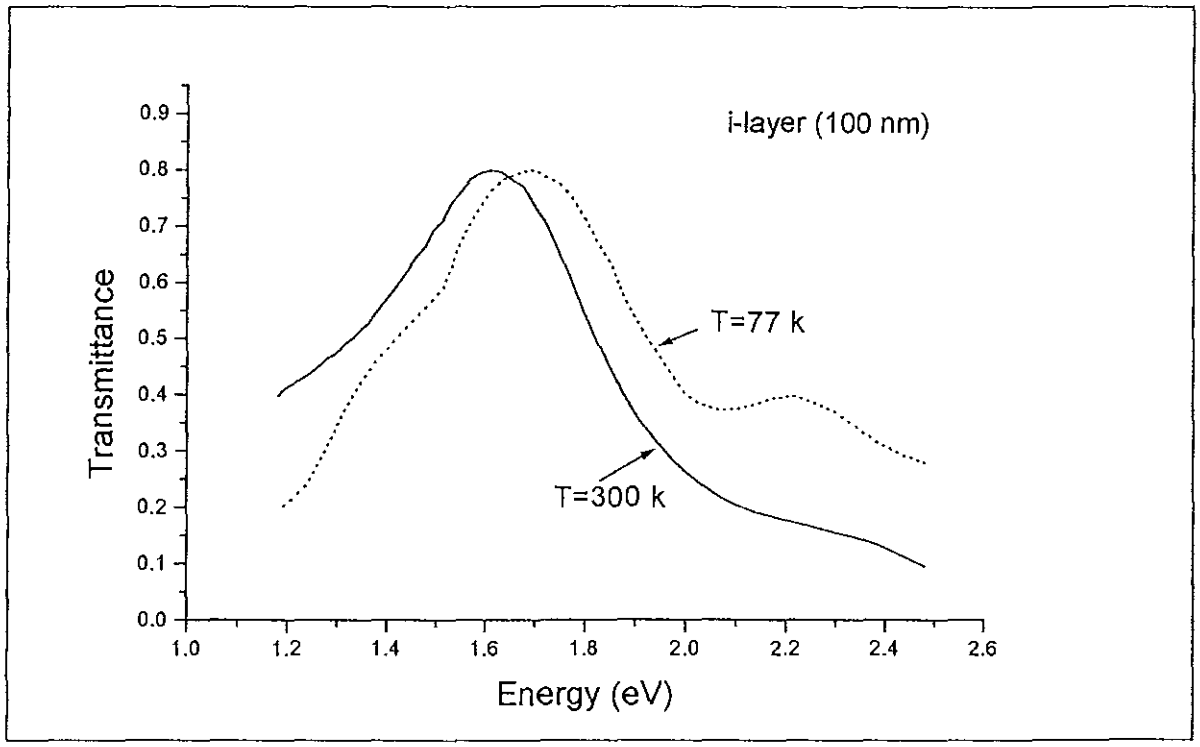

Fig. 8.1 The transmittance spectra of a thin i-layer a-Si:H film of thickness 100 nm at 77 k (dotted line) and 300 K (solid line).

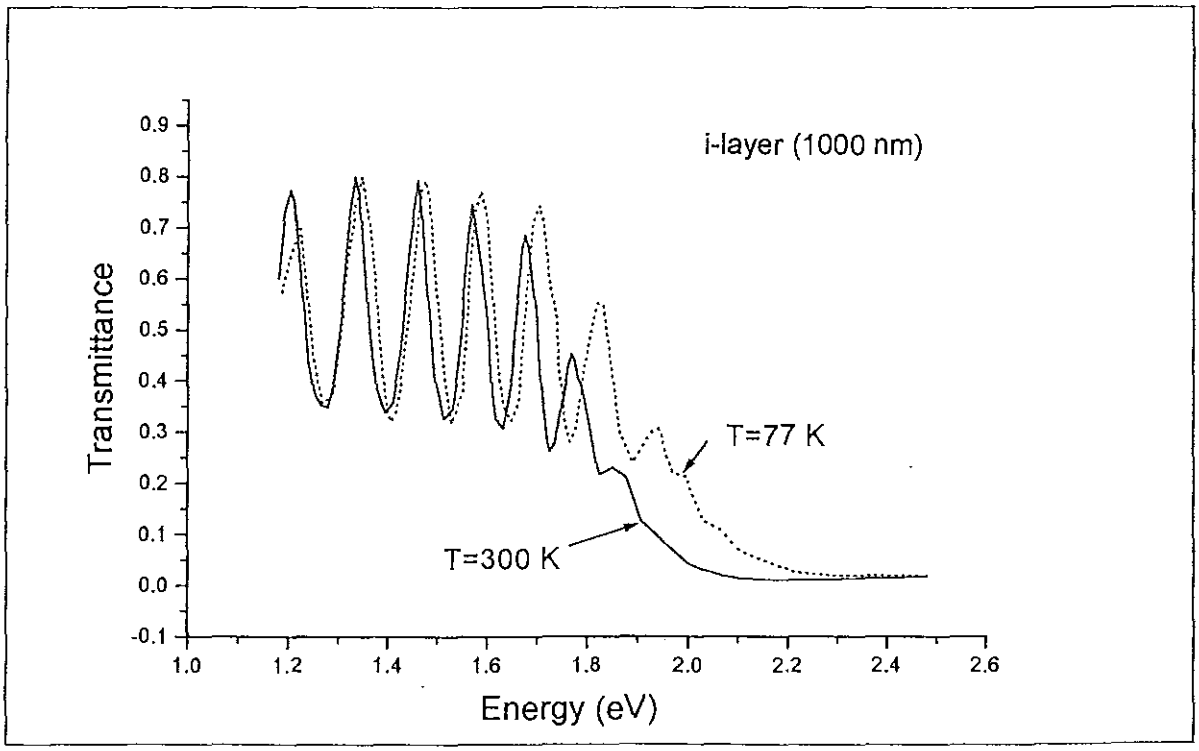

Fig. 8.2 The transmittance spectra of i-layer a-Si:H film of thickness 1000 nm at 77 K (dotted line) and 300 K (solid line).

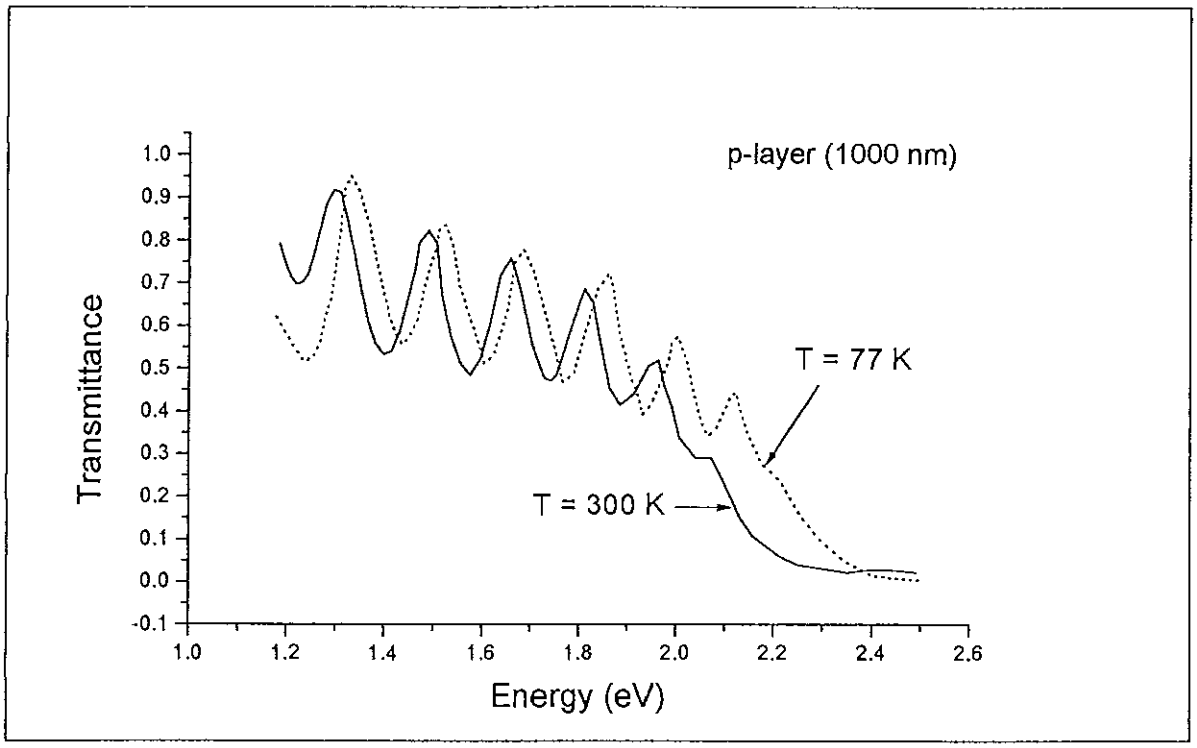

Fig. 8.3 The transmittance spectra at 77 K (dotted line) and 300 K (solid line) of a p-layer a-Si:H thin film of thickness 1000 nm.

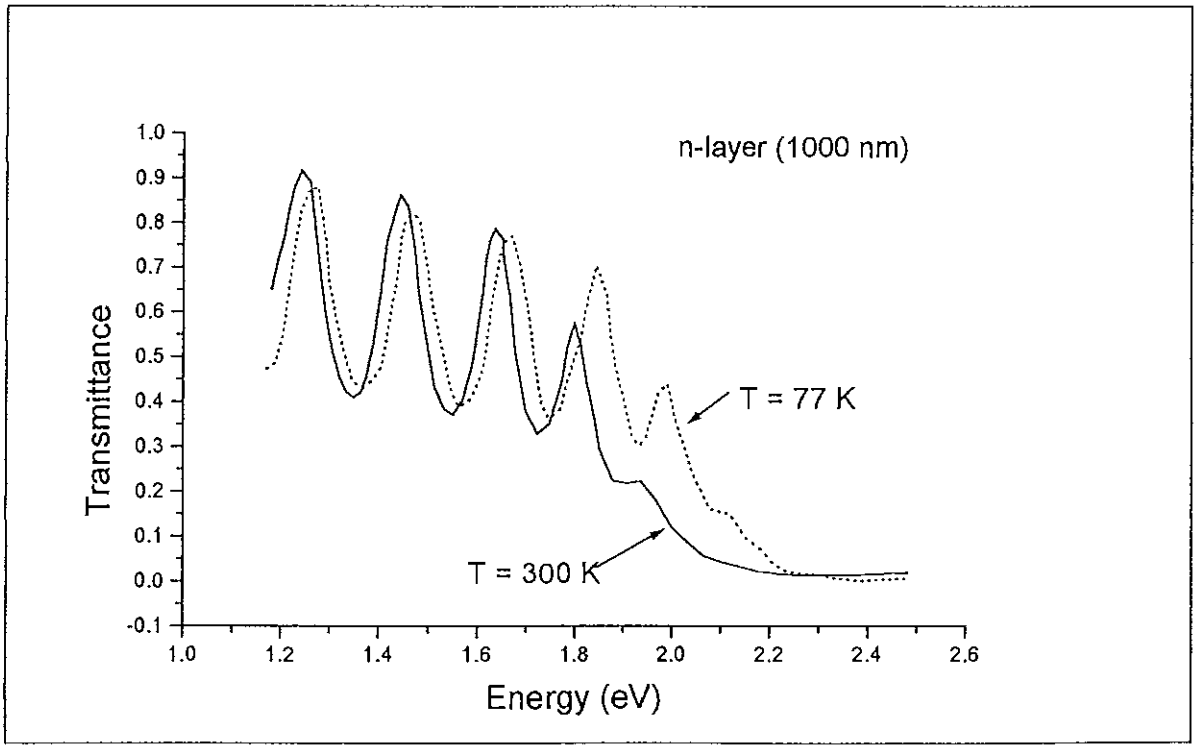

Fig. 8.4 The transmittance spectra at 77 K (dotted line) and 300 K (solid line) of an n-layer a-Si:H film of thickness 1000 nm.

8.2 The Shift of the Optical Band Gap of a-Si:H Thin Films with Temperature.

Figure 8.5 shows the measured (solid line) and simulated (doted line) transmittance spectra for the thin i-layer a-Si:H thin film sample of thickness 100 nm at sample temperature of 77 K. As calculated by the SCOUTFIT program the energy gap obtained is 1.6301 eV with a χ^2 deviation of 0.0006118. In Fig. 8.6 the measured and simulated transmittance spectra for the thin i-layer at 300 K are depicted. Again a good agreement between the two curves specially in the region of interest with χ^2 deviation of 0.0004926 is obtained. At 300 K the optical band gap obtained for the thin i-layer is 1.5474 eV. This result is comparable with values given in literature [10, 22]. There is a decrease in the energy gap with increasing temperature. The decrease in the optical band gap observed for this sample when the temperature is increased from 77 K to 300 K is 0.0827 eV.

Figures 8.7 and 8.8 show the transmittance spectra for the thick i-layer film of thickness 1000 nm at sample temperatures of 77 K and 300 K respectively. The χ^2 deviation between the measured and simulated transmittance spectra were 0.000653 at 77 K and 0.0006443 at 300 K. The optical band gaps calculated at 77 K and 300 K are respectively 1.645 eV and 1.5573 eV, and the energy band gap shift when the temperature is increased from 77 K to 300 K is -0.0877 eV.

Even if the two i-layers discussed above are different in thickness, since they are prepared under the same conditions, the energy gaps and the temperature shifts in the energy gaps are nearly the same for both intrinsic a-Si:H films.

The measured (solid line) and fitted (dotted line) transmittance spectra are shown for the p-layer a-Si:H thin film sample at 77 K in Fig. 8.9 and at 300 K in Fig. 8.10, with χ^2 deviation 0.001106 at 77 K and 0.000964 at 300 K. The optical band gaps obtained from the

SCOUTFIT program are 1.9596 eV at 77 K and 1.876243 eV at 300 K. For this layer it can be observed again that the optical band gap is larger at the lower temperature and the decrease in the band gap observed by increasing the temperature from 77 K to 300 K is 0.0833 eV.

For the n-layer sample presented in Figs. 8.11 and 8.12 the χ^2 deviation were 0.0008759 at 77 K and 0.00115 at 300 K. The optical band gaps calculated are 1.7996 eV at 77 K and 1.7302 eV at 300 K and the decrease in the energy gap with increasing temperature is 0.0694 eV.

The optical parameters for the p-, i- and n- layer a-Si:H thin film samples obtained by simulation are listed in Table 8.1. Table 8.2 shows the comparison of the optical parameters with reference values for similar samples. Comparison of the thickness of the glass substrate is made with the value measured using a micrometer. For all the samples the optical band gaps obtained by the SCOUTFIT program with applied Forouhi and Bloomer dielectric function model are in good agreement with results from literature [10, 22], for similar samples with a deviation of about +/- 6.23 % (see Table 8.2). For the observed GD a-Si:H thin film samples the energy gap decreases as temperature increases, which is consistent with literature [11, 16, 24]. Table 8.3 lists the optical band gaps obtained for each a-Si:H thin film samples investigated at the two temperatures (77 K and 300 K) and the shift of the optical band gap with increasing temperature.

The deviations observed from the comparison of the optical band gaps and their shift with temperature obtained in this investigation with values from references [16, 25] were shown in Tables 8.2 and 8.3. Some of the main sources of these deviations could be: The fluctuation of the transmission intensity which reaches up to +/- 6.3 % that is observed mainly during measurement with liquid nitrogen; the relatively low resolution of the monochromator which is about +/-0.0124 eV at 500 nm and the dependence of the detectivity of the photodiode with photon energy. Furthermore, the optical band gap of a-Si:H depends on the details of the

preparation conditions [11], this can also contribute to the observed deviations of the optical band gaps of the investigated a-Si:H thin film samples with reference values.

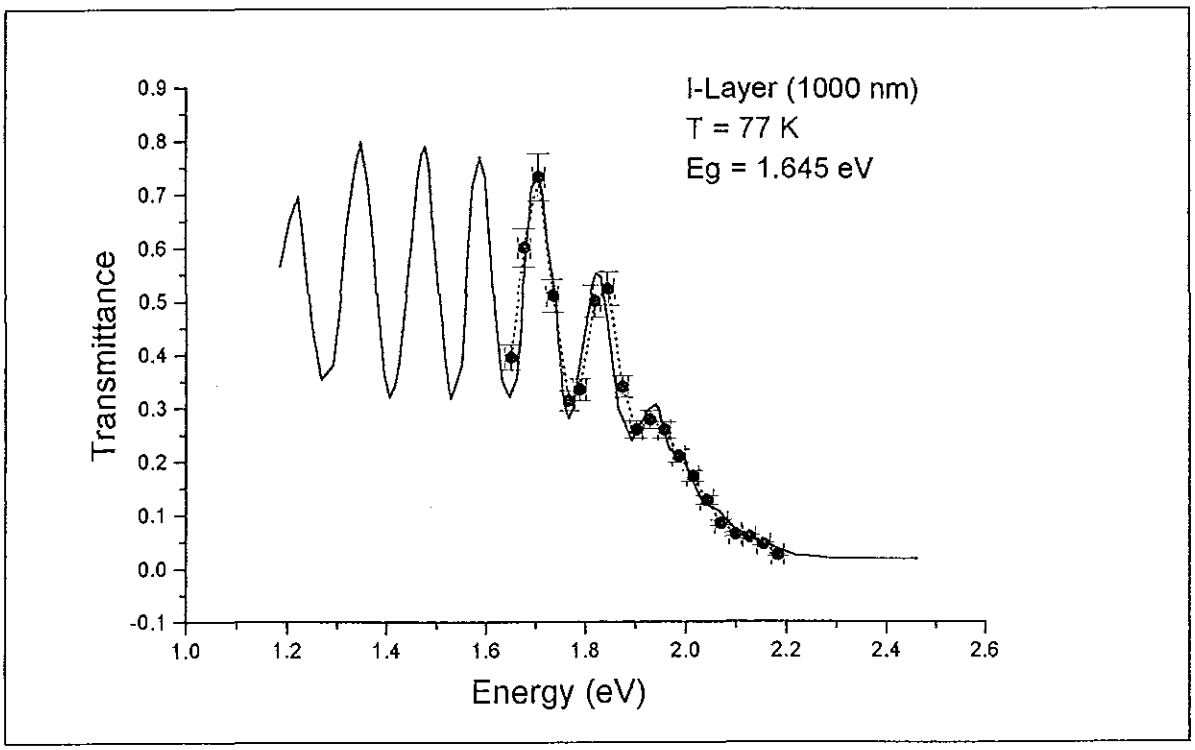

Fig. 8.7 Measured (solid line) and SCOUTFIT simulated (dotted line) transmittance spectra of i-layer a-Si:H thin film of thickness 1000 nm at 77 K.

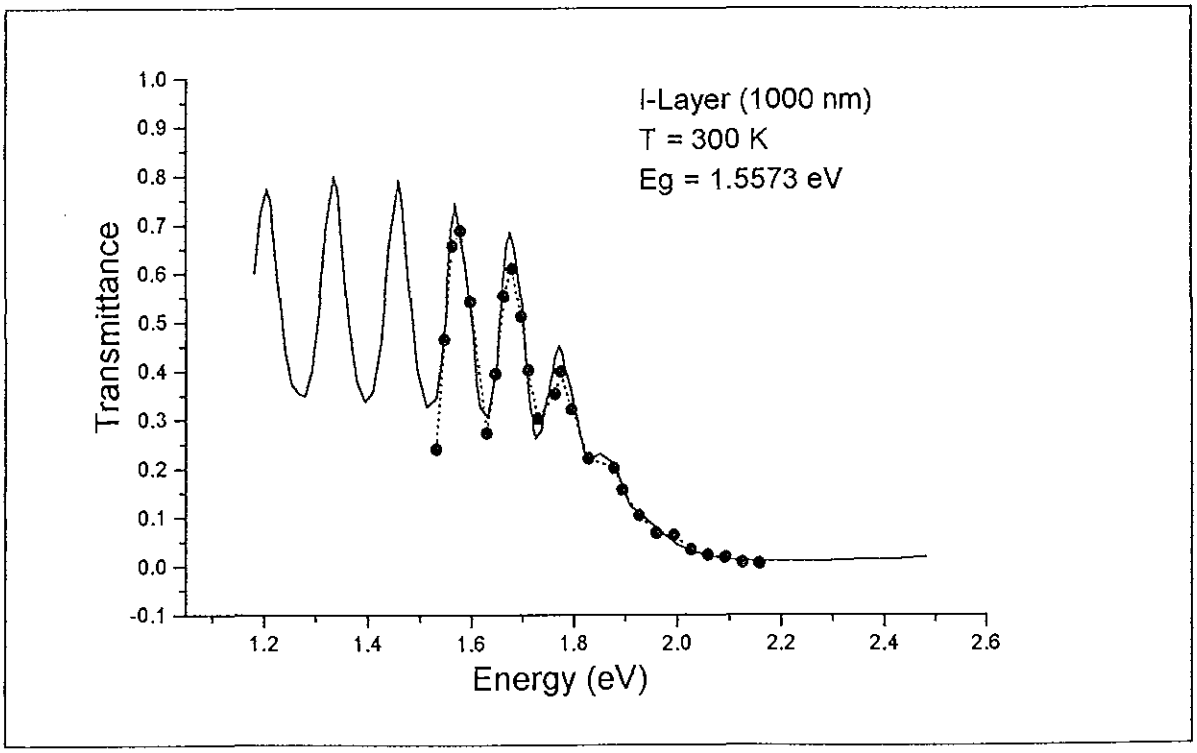

Fig. 8.8 Measured (solid line) and simulated (dotted line) transmittance spectra of i-layer a-Si:H thin film of thickness 1000 nm at 300 K.

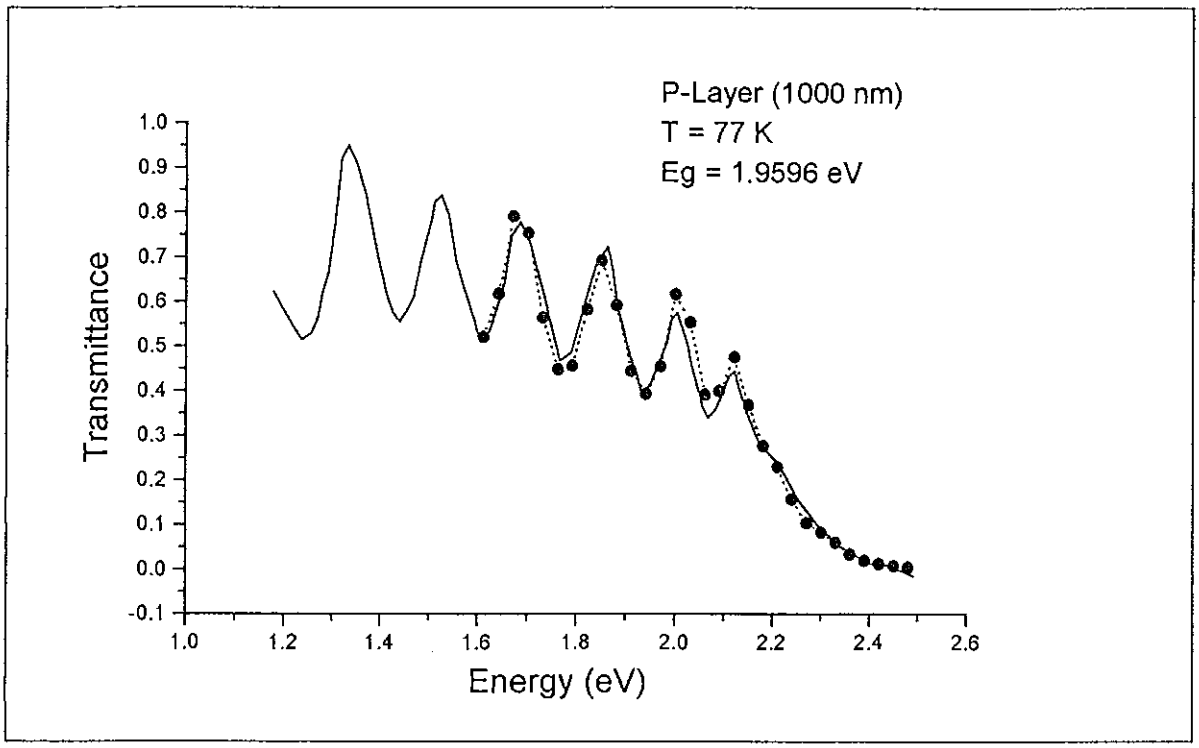

Fig. 8.9 Measured (solid line) and simulated (dotted line) transmittance spectra of p-layer a-Si:H thin film of thickness 1000 nm at 77 K.

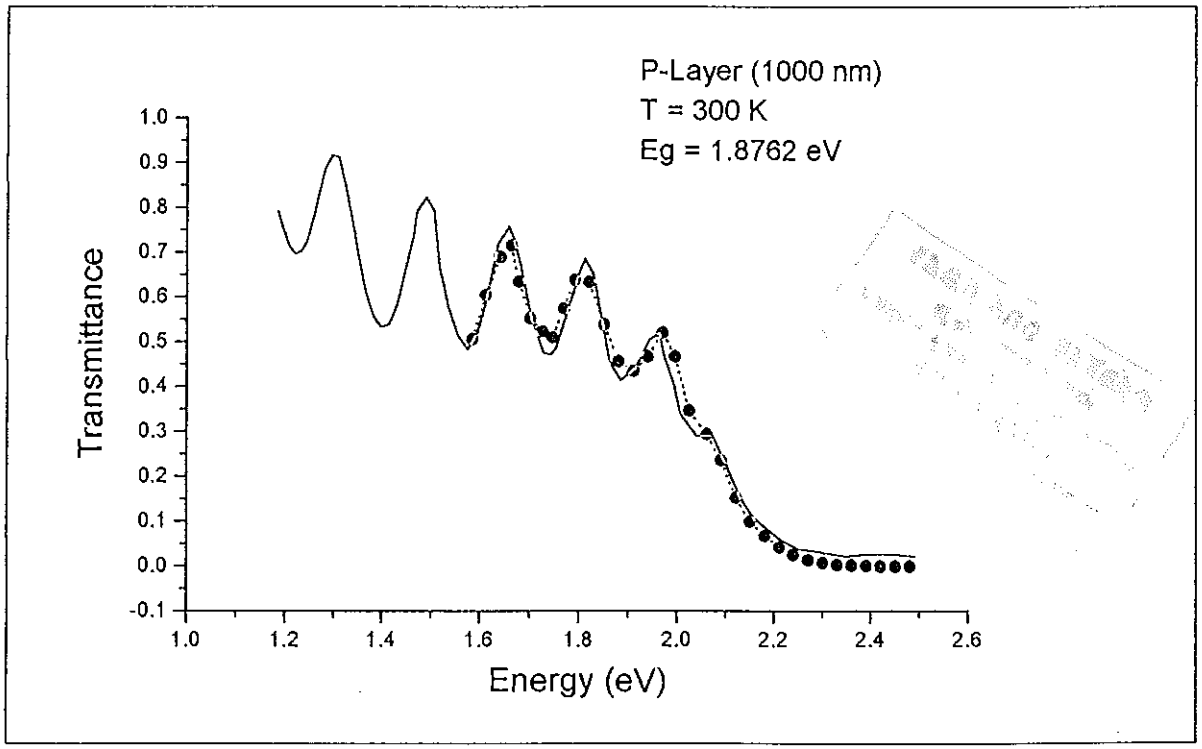

Fig. 8.10 Measured (solid line) and simulated (dotted line) transmittance spectra of p-layer a-Si:H thin film of thickness 1000 nm at 300 K.

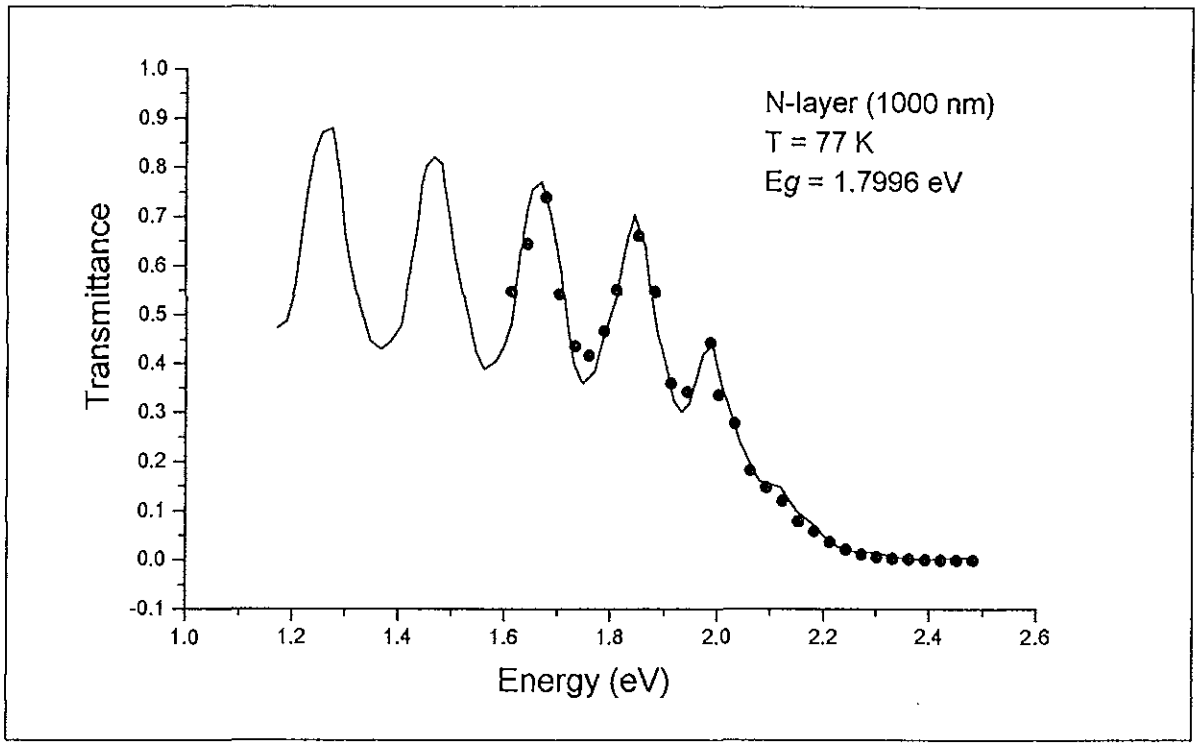

Fig. 8.11 *Measured (solid line) and simulated (dotted line) transmittance spectra of n-layer a-Si:H thin film of thickness 1000 nm at 77 K.*

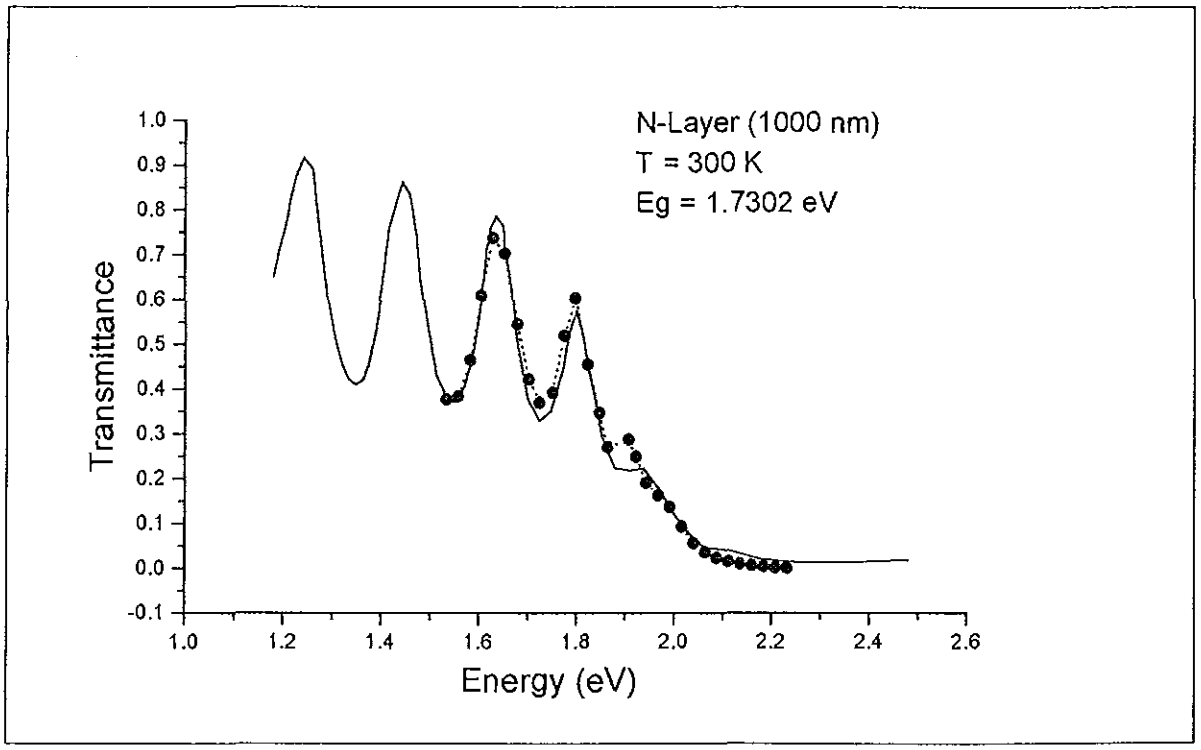

Fig. 8.12 Measured (solid line) and simulated (dotted line) transmittance spectra of n- layer a-Si:H thin film of thickness 1000 nm at 300 K.

Table 8.1 Optical constants obtained by simulation of the measured transmittance spectra at 77K and 300K.

system	parameters	dimension	77K	300K
Glass	ε_{inf}		2.472/2.86/2.0514/2.14	2.1532/2.3425/1.89/2.73
	d	μm	1289.2/1186.2/1385.34/1019	1010.9/1199.78/1189/962
TCO	ε_{inf}		4.187/3.6835/3.7431/4.51	2.99/3.0786/4.52/3.74
	d	μm	0.0531/0.0476/0.0808/0.072	0.0736/0.082/0.06/0.082
Thin i-layer	A		1.44358	1.83252
	B	eV	5.2927	6.0113
	C	$(eV)^2$	10.329	11.23
	n_{inf}		3.982	3.1853
	E_g	eV	1.6301	1.54742
	d	μm	0.0726	0.0958
thick i-layer	A		1.51061	1.34465
	B	eV	5.5388	5.7864
	C	$(eV)^2$	9.253	7.334
	n_{inf}		2.513	2.822
	E_g	eV	1.645	1.5573
	d	μm	0.9725	1.0291
p-layer	A		1.2377	1.7031
	B	eV	5.6943	4.847
	C	$(eV)^2$	8.287	8.989
	n_{inf}		3.42	3.13
	E_g	eV	1.9596	1.87624
	d	μm	0.9629	1.0003
n-layer	A		1.721	1.633
	B	eV	6.0267	4.0613
	C	$(eV)^2$	10.7436	7.582
	n_{inf}		3.768	3.1894
	E_g	eV	1.7996	1.7302
	d	μm	1.1266	0.9308

Table 8.3 Optical band gaps obtained at the two measuring temperatures (77K and 300K).

sample	E_g(77K)	E_g(300K)	ΔE_g		deviation [%]
			measured	reference	
i-layer	1.63375	1.55236	-0.08519	-0.08[16]	6.5
p-layer	1.9596	1.87624	-0.0833	-0.058[24]	29.76
n-layer	1.7996	1.7302	-0.0694	-0.06[24]	15.7

9. Conclusion

The transmittance spectra measured for each p-, i-, and n-layer a-Si:H thin film samples at temperatures of 77 K and 300 K show a temperature shift towards lower energies with increasing temperature. Near the spectral region of the optical band gap of the films the observed temperature spectral shift ranges from 0.05 eV to 0.09 eV. As an additional evidence for the temperature shift of the optical band gap towards lower energies with increasing temperature, it is observed that in the region where absorption is strong the transmission decreases with increasing temperature.

The optical band gaps calculated by the computer simulation using the SCOUTFIT program at both temperatures show a good agreement with reference values obtained for similar samples with deviation of about +/-6.23 %. For the investigated a-Si:H thin film samples the observed change in the optical band gap with increasing temperature (from 77 K to 300 K) is in the range of 0.0694 eV to 0.08519 eV. For quantitative comparison with theoretically derived equations of $E_g(T)$ more then two experimentally available temperatures are required. The further development in the design of the glass tube liquid nitrogen cryostat to establish temperatures in-between 77 K and 300 K would be a promising project for the Physics Department of the AAU in the near future.

Since the open circuit voltage V_{oc} and the short circuit current J_{sc} change with temperature [4, 25], the knowledge of the optical band gap as a function of temperature $E_g(T)$ will give additional information for a detailed interpretation of $V_{oc}(T)$, $J_{sc}(T)$, fill factor FF(T) and $\eta(T)$ for a-Si:H p-i-n solar cells.

References

[1] S. R. Elliot, "Physics of Amorphous Materials", Second Edition, Department of Physical Chemistry, University of Cambridge, Longman Scientific and Technical, New York, (1990).

[2] S. J. Hudgens, Physical Considerations in the Design of Multi-Junction Amorphous Silicon Alloy Solar Cells, First International Symposium on Physics and Application of Amorphous Semiconductors, World Scientific, Singapore (1987).

[3] D. Adler, B. B. Schwartz and M. C. Steele, "Physical Properties of Amorphous Materials," Institute for Amorphous Studies Series, Plenum Press, New York (1985).

[4] M. H. Broadsky, Topics in Applied Physics, Springer, Berlin, Vol. 36 (1985).

[5] E. A. Davis, Electronic Properties of Non-Crystalline Semiconductors, Physics and Chemistry of Electrons and Ions in Condensed Matter, NATO ASI Series, D. Reidel Publising, Holland, pp. 145-163 (1984).

[6] B. Sapoval C. Hermann, Physics of Semiconductors, Springer, Berlin (1995).

[7] M. V. Klein and T. E. Furtak, "OPTICS", Second Edition, John Wiley & Sons, New York (1986).

[8] W. Theiss, The Scout Through CAOS, A System for Doing Optics by Computer, SCOUTFIT 94 Computer Programme Manual (1994).

[9] A. R. Forouhi and I. Bloomer, Phys. Rev. B, Vol. 38, No. 3, pp. 1865-1874 (1988).

[10] A. R. Forouhi and I. Bloomer, Phys. Rev. B, Vol. 34, No. 10, pp. 7018-7025 (1986).

[11] K. Tankana and S. Yamasaki, Optical Absorption Edge of Hydrogenated Amorphous Silicon, Disordered Semiconductors, Institute of Amorphous Study Series, Plenum, New York, pp. 425-434 (1987).

[12] A. Madan and M. P. Shaw, "The Physics and Application of Amorphous Semiconductors", Academic Press, Boston (1988).

[13] A. R. Forouhi and I. Bloomer, Hand Book of Optical Constants of Solids II, Academic Press, London, pp. 151-175 (1991).

[14] K. W. Boer, Survey of Semiconductor Physics, Electrons and Other Particles in Bulk Semiconductors, Van Nostrand Reinhold, New York (1990).

[15] T. D. Moustakas, The Role of Hydrogen in Trace Impurity Doping of Amorphous Silicon, First International Symposium on Physics and Applications of Amorphous Semiconductors, World Scientific, Singapore, pp. 399-403 (1987).

[16] G. D. Cody, T. Tiedje, B. Abeles, B. Brooks, and Y. Goldstein, Phys. Rev. Lett. Vol. 47, No. 20, pp. 1480-1483 (1981).

[17] S. Oda, H. Shirai, A. Tanabe, J. Hanna and I. Shimizu, Material Design by Structural Modulation of Amorphous Semiconductors, Disordered Semiconductors, Institute of Amorphous Study Series, Plenum, New York, pp. 563-575 (1987).

[18] D. A. Neamen, Semiconductor Physics and Devices, Irwin, Boston (1992)

[19] R. E. Hummel, Electronic Properties of Materials, Second Edition, Springer, Berlin, pp. 182-184 (1993).

[20] U. Stutenbaeumer, Belayneh Mesfin and Solomon Beneberu, Determination of Optical Constants and the Dielectric Functions of Thin Film a-Si:H Solar Cell Layers, to be published (1998).

[21] R. Plaettner, W. Stettner, P. Koehler, Transparent Conductive Tin Oxide Layers for Thin Film Solar Cells. In: Siemens Forch.-u. Entwickl.- Ber. 17, No 3, pp. 126 (1998).

[22] T. Eickhoff, and H. Stiebig, Modellierung der Spektralen Empfindlichkeit Von a-Si:H Solarzellen. Photovoltaic 3 (1996).

[23] R. J. Schwartz, G. B. Turner, J. W. Park and J. L. Gray, Physics of Amorphous Semiconductor Devices, Vol. 763, pp. 126 (1987).

[24] Challa Bekele, Temperature Dependence of the Optical Properties of a-Si:H Thin Films for Solar Cells, Thesis (AAU) (1996).

[25] Th. Eickhoff, H. Stiebig, W. Reetz, B. Rech and H. Wagner, Temperature Dependence of a-Si:H Solar Cell Parameters-Experiments and Numerical Simulation, 13th E. C Photovoltaic Solar Energy Conference, Nice (1995).